NASA Technical Memorandum 84324

Efficient Algorithms for Computing Trim and Small-Disturbance Equations of Motion of Aircraft in Coordinated and Uncoordinated, Steady, Steep Turns

Robert T. N. Chen

February 1983

NASA
National Aeronautics and
Space Administration

NASA Technical Memorandum 84324

Efficient Algorithms for Computing Trim and Small-Disturbance Equations of Motion of Aircraft in Coordinated and Uncoordinated, Steady, Steep Turns

Robert T. N. Chen, Ames Research Center, Moffett Field, California

NASA
National Aeronautics and
Space Administration

Ames Research Center
Moffett Field, California 94035

SUMMARY

The development of computational algorithms that permit efficient calculation of aircraft trim states and of the associated small-disturbance equations of motion for a systematic investigation of the statics and dynamics of aircraft in coordinated and uncoordinated, steady, steep-turning flight is reported. The efficiency in the trim computation is realized by decoupling the governing equations. The small-disturbance equations of motion, which are given in a general body-axis system, include aerodynamic acceleration derivatives; they are cast in a familiar first-order, vector-matrix format of modern system theory. These algorithms have been applied to a variety of rotorcraft simulation models. Results pertaining to a simulated hingeless-rotor helicopter are also presented.

INTRODUCTION

Steep turns at low speeds, particularly in adverse wind conditions have presented severe flight dynamic problems for both fixed-wing and rotary-wing aircraft. For example, a recent review (ref. 1) indicates that many stall/spin accidents in general aviation aircraft involve steep turns at low speeds (thus, high angle of attack). A study by the Army has also indicated that many Army helicopter mishaps that are attributable to loss of directional control through tail-rotor stall involve steep turns at low speeds (thus high thrust of the tail rotor) (ref. 2). To provide a basis for better understanding these problems and other generic characteristics involving aircraft in extreme asymmetric flight, there is a need to develop a new analytical framework and associated analytical tools for theoretical investigations and experimental correlations.

Traditionally, the standard equations of airplane motion for small-disturbances from steady, symmetrical, straight 1-g flight as the reference flight condition (refs. 3, 4) have been the basis for stability and control analyses, flying-qualities specifications (refs. 5-8), and design analyses of stability and control augmentation systems (SCAS) for fixed-wing and rotary-wing aircraft. However, for an aircraft that performs such extreme asymmetric maneuvers as steep, high-g turns, flying-qualities designs based on small-disturbances from steady straight flight may be grossly inadequate. A new analytical procedure is required, one that permits using steady-asymmetrical, curved, high-g flight as a reference flight condition for systematic examinations of the flight dynamics and control characteristics of the basic aircraft and its SCAS to ensure that the overall aircraft-SCAS system will perform satisfactorily, not only in operations near 1-g flight but also in high-g maneuvers.

Toward meeting this need, a step was previously taken (refs. 9, 10) to develop algorithms that permit efficient computations of aircraft states and control positions in coordinated, steady, steep turns and the associated small-disturbance equations of motion. In developing these algorithms, special emphasis was placed on considerations of the inherent sideslip which normally exists in an asymmetric aircraft, such as a single-rotor helicopter, in coordinated flight. Using these algorithms, a study was recently conducted to investigate the statics and flight dynamics of several rotorcraft in coordinated, steep, high-g turns (ref. 11). The results of that study indicate (1) that strong coupling in longitudinal and lateral-directional motions exists for rotorcraft in coordinated, high-g turns; (2) that for single-rotor helicopters the direction of turn has a significant influence on flight dynamics; and (3) that an SCAS that is designed on the basis of standard small-disturbance equations

of motion from steady straight and level flight and that otherwise performs satisfactorily in operation near 1-g, becomes significantly degraded in steep turning flight.

To expand the basis for broader applications, the algorithms previously developed (refs. 9, 10) have been extended to permit efficient trim computations of uncoordinated flight, both uncoordinated steep turns and uncoordinated straight flight. This report presents that generalization and describes some results of applying these generalized algorithms to rotorcraft.

NOMENCLATURE

g	gravitational acceleration
I_x	moment of inertia about x-body axis
I_{xz}, I_{yz}, I_{xy}	product of inertias in body axes
I_y	moment of inertia about y-body axis
I_z	moment of inertia about z-body axis
L	total aerodynamic and propulsive moment about x-body axis
M	total aerodynamic and propulsive moment about y-body axis
m	aircraft mass
N	total aerodynamic and propulsive moment about z-body axis
n	ratio of the total aerodynamic and propulsive force acting on the aircraft to the weight of the aircraft
n_T	ratio of the total aerodynamic and propulsive force acting on the aircraft perpendicular to the flightpath to the weight of the aircraft
n_x, n_y, n_z	accelerometer reading along the body axes (also referred to as n-parameters along the body axes)
p, q, r	angular rates of the aircraft about body axes
u, v, w	airspeed components in the aircraft body axes system
V	airspeed
X	total aerodynamic and propulsive force acting on the aircraft along x-body axis
x, y, z	body axes system
Y	total aerodynamic and propulsive force acting on the aircraft along y-body axis

Z	total aerodynamic and propulsive force acting on the aircraft along z-body axis
α	angle of attack with respect to air mass, $\alpha \triangleq \tan^{-1}(w/u)$
β	angle of sideslip with respect to air mass, $\beta \triangleq \sin^{-1}(v/V)$
γ	aircraft flightpath angle
$\delta_a, \delta_c, \delta_e, \delta_p$	lateral, collective, longitudinal, and directional control displacements, respectively
Φ, Θ, Ψ	aircraft Euler angles
ϕ_1	tilt angle of the $\vec{n}_T$ from the vertical plane containing the flightpath
$\dot{\Psi}$	rate of turn of the aircraft about Earth-referenced vertical axis

Subscript:

0	value at the steady flight conditions

EQUATIONS GOVERNING AIRCRAFT IN STEADY, UNCOORDINATED, HELICAL TURNS

A set of kinematic equations (see table 1) governing an aircraft in a steady, coordinated helical turn about a vertical axis was previously given in references 9 and 10. In that development, special consideration was given to the existence of an inherent sideslip — which is usually the case for single-rotor helicopters, in a coordinated turn. The development was consistent with the flat-Earth approximation and used no small-angle assumptions. For a more general case of a steady, uncoordinated, helical turn, the governing equations (as shown in table 1) must be slightly modified. The steady-state Euler equations (1) and the kinematic equations (2) in table 1, which are related to the aircraft attitudes and angular rates are the same as equations (1) and (2) below (repeated here for convenience) except that equation (2a) below is different from (2a)' in table 1:

$$\frac{X}{mg} - \sin\Theta - \tan\phi_1(\sin\alpha\cos\beta\cos\Theta\sin\Phi - \sin\beta\cos\Theta\cos\Phi) = 0 \qquad (1a)$$

$$\frac{Y}{mg} + \cos\Theta\sin\Phi - \tan\phi_1\cos\beta(\cos\alpha\cos\Theta\cos\Phi + \sin\alpha\sin\Theta) = 0 \qquad (1b)$$

$$\frac{Z}{mg} + \cos\Theta\cos\Phi + \tan\phi_1(\sin\beta\sin\Theta + \cos\alpha\cos\beta\cos\Theta\sin\Phi) = 0 \qquad (1c)$$

$$L + I_{yz}(q^2 - r^2) + I_{xz}pq - I_{xy}rp + (I_y - I_z)qr = 0 \qquad (1d)$$

$$M + I_{xz}(r^2 - p^2) + I_{xy}qr - I_{yz}pq + (I_z - I_x)rp = 0 \qquad (1e)$$

$$N + I_{xy}(p^2 - q^2) + I_{yz}rp - I_{xz}qr + (I_x - I_y)pq = 0 \qquad (1f)$$

$$\sin \Phi = \tan \phi_1 (\cos \alpha \cos \Phi + \sin \alpha \tan \Theta) \cos \beta - n_y / \cos \Theta \tag{2a}$$

$$\sin \gamma = \cos \alpha \cos \beta \sin \Theta - (\sin \beta \sin \Phi + \sin \alpha \cos \beta \cos \Phi) \cos \Theta \tag{2b}$$

$$p = -\dot{\Psi} \sin \Theta \tag{2c}$$

$$q = \dot{\Psi} \cos \Theta \sin \Phi \tag{2d}$$

$$r = \dot{\Psi} \cos \Theta \cos \Phi \tag{2e}$$

In the above equations, the turn parameter ϕ_1 is the tilt angle of the acceleration normal to the flightpath from the vertical plane. It can be expressed in terms of the turn rate $\dot{\Psi}$, the normal load factor n_T, and the total load factor n, respectively, as follows:

$$\phi_1 = \tan^{-1} \left(\frac{\dot{\Psi} V}{g} \right) \tag{3a}$$

$$= \pm \tan^{-1} \left[\frac{(n_T^2 - \cos^2 \gamma)^{1/2}}{\cos \gamma} \right] \tag{3b}$$

$$= \pm \tan^{-1} \left[\frac{(n^2 - 1)^{1/2}}{\cos \gamma} \right] \tag{3c}$$

where the positive signs in equations (3b) and (3c) are for right turns and the negative signs for left turns. It should be noted here that equations (3) apply to uncoordinated flight ($n_y \neq 0$), as well as coordinated flight ($n_y = 0$), as discussed previously in references 9 and 10. These 11 algebraic equations (eqs. (1) and (2)) completely determine the 11 unknown trim values of the aircraft flight parameters, that is, the Euler attitudes Θ, Φ; body-axis angular rates p, q, r; angle of attack α; angle of sideslip β; and the four control variables of the aircraft. Note that the side force $Y = n_y mg$ in equations (1) is known since n_y is specified. The value of n_y signifies the extent to which the flight is out of coordination.

As will be discussed at some length later, the determination of the trim values can be greatly simplified by solving for the aircraft attitudes Θ and Φ, and the body-axis angular rates p, q, and r in terms of the turn parameters V, γ, $\dot{\Psi}$ (or n_T), and the angles of attack and sideslip, thereby decoupling the 11 governing equations. A solution to achieve this desired purpose was obtained in reference 9 for the case of steady, coordinated, helical turns. An extension to the case of uncoordinated, helical turns is achieved as described in the appendix of this report. The resulting closed-form solutions are as follows:

$$\left.\begin{aligned} q &= \dot{\Psi} \sin^2 \phi_1 \left\{ - (\sin \gamma \sin \beta + n_y \cot^2 \phi_1) \right. \\ &\quad \left. \pm \left[(\sin \gamma \sin \beta + n_y \cot^2 \phi_1)^2 - \frac{1}{\sin^2 \phi_1} (\sin^2 \gamma - \cos^2 \beta + n_y^2 \cot^2 \phi_1) \right]^{1/2} \right\} \\ q &\geq 0 \\ r' &= \frac{q + \dot{\Psi} n_y}{\tan \phi_1 \cos \beta} \end{aligned}\right\} \tag{4}$$

$$\left.\begin{aligned} p' &= -\frac{\dot{\Psi}\sin\gamma}{\cos\beta} - q\tan\beta \\ p &= p'\cos\alpha - r'\sin\alpha \\ r &= p'\sin\alpha + r'\cos\alpha \\ \Theta &= \sin^{-1}(-p/\dot{\Psi}) \\ \Phi &= \tan^{-1}(q/r) \end{aligned}\right\} \qquad (4) \text{ (cont)}$$

When n_y is zero, a turn becomes coordinated, and the equations in (4) reduce, as they should, to those previously obtained in reference 9. The set of formulas in (4) may also provide a basis for a thorough examination of the kinematic properties of the aircraft in steady uncoordinated turns without having to consider its detailed aerodynamic characteristics.

For straight flight, coordinated or otherwise, the rate of turn vanishes ($\dot{\Psi} = 0$). Under this condition, the body-axis angular rates p, q, and r are identically zero and the computational formulas for aircraft pitch and roll attitudes in equations (4) become indefinite. However, for this singular case, the aircraft attitudes can be computed, as described in the appendix, using the following formulas:

$$\Theta = \sin^{-1}\left\{\frac{\cos\alpha(\sin\gamma - n_y\sin\beta) + \sin\alpha[\cos^2\beta - \sin^2\gamma + n_y(2\sin\beta\sin\gamma - n_y)]^{1/2}}{\cos\beta}\right\} \qquad (5)$$

$$\Phi = \sin^{-1}\left(\frac{-n_y}{\cos\Theta}\right) \qquad (6)$$

Note that when $n_y = 0$, equations (5) and (6) reduce to

$$\left.\begin{aligned} \Theta &= \sin^{-1}\left(\frac{\sin\gamma}{\cos\beta}\right) + \alpha \\ \Phi &= 0 \end{aligned}\right\} \qquad (7)$$

which have previously been given in reference 9. For convenience, the key equations in this section are summarized in table 2.

Before closing this section it should be emphasized that throughout the development presented in this report, the aircraft center of gravity is used as the reference point for describing all the flight parameters. Thus, n_y, for instance, is the accelerometer reading along the y-body axis with origin at the center of gravity of the aircraft. The accelerometer (and vane) signals depend on sensor location relative to the aircraft center of gravity. For example, if an accelerometer is mounted at the instrument panel and is denoted by the vector $\vec{r} = (x, y, z)$ with the designated body-axis components relative to the aircraft center of gravity, its signals along the y-body-axis n_{y_r} in a steady turn will be

$$n_{y_r} = n_y + \frac{1}{g}[qrz - (r^2 + p^2)y + pqx]$$

where the additional terms on the right-hand side of the above equation are the required correction for its location to account for the angular rates of the aircraft about its center of gravity.

TRIM COMPUTATION

The new formulas (4) which directly connect the aircraft angular rates and pitch and roll attitudes to the turn parameters and to the angles of attack and sideslip can be used to drastically simplify the trim computation for the helicopter in a steady, coordinated, helical turn. These formulas essentially decouple the 11 governing equations (1) and (2).

For a steady, helical turn, the 11 governing equations in table 2 uniquely determine the trim values of the following 11 flight parameters:

Angles of attack and sideslip	α, β
Aircraft angular rates	p, q, r
Aircraft pitch and roll attitudes	Θ, Φ
Control positions, for example,	δ_a, δ_c, δ_e, δ_p

It would be necessary, without the five new formulas (4) for aircraft angular rates and pitch and roll attitudes, to invert an associated 11 × 11 Jacobian matrix in each iterative cycle in the numerical solution of the 11 (nonlinear algebraic) governing equations. With the aircraft angular rates and Θ and Φ expressed explicitly in terms of α and β, the associated Jacobian matrix can be compressed into a simpler 6 × 6, as normally is the case for a steady straight-flight condition.

Let c, f, and g be denoted by

$$\left.\begin{aligned} c &= (\alpha,\ \beta,\ \delta_a,\ \delta_c,\ \delta_e,\ \delta_p)^T \\ f &= (f_1,\ f_2,\ f_3,\ f_4,\ f_5,\ f_6)^T \\ g &= (p,\ q,\ r,\ \Theta,\ \Phi)^T \end{aligned}\right\} \tag{8}$$

where $f_1, f_2, \ldots, f_6$ are the first six steady-state Euler equations in table 2. Note that $g = g(c)$. Then f takes the form

$$f = F[c,\ g(c)] = 0 \tag{9}$$

The associated 6 × 6 Jacobian matrix $\partial f/\partial c$ becomes

$$\frac{\partial f}{\partial c} = \frac{\partial F}{\partial c} + \frac{\partial F}{\partial g}\frac{\partial g}{\partial c} \tag{10}$$

The Jacobian matrix $\partial f/\partial c$ is a necessary ingredient in the iterative methods for numerical solution of the trim equations. If, for example, a Newtonian-type procedure

is used, then an algorithm for determining the trim values for the vector c beginning with an initial guess c_o is of the following kind:

$$c_{i+1} = c_i + \delta c_i \tag{11a}$$

$$\delta c_i = -\lambda_i \left(\frac{\partial f}{\partial c_i}\right)^{-1} f(c_i) \tag{11b}$$

where $\lambda_i \leq 1$ is a damping parameter for a stable iteration. With the trim value for c determined, say c_t, the desired trim values for the angular rates and Θ and Φ follow immediately, which are

$$g_t = g_t(c_t) \tag{12}$$

Experience in applying this trim algorithm to a variety of rotorcraft simulation mathematical models has indicated that an appropriate initial guess c_o to initiate the trim computation is to use its 1-g flight trim value. With this initial guess, and provided that the specified steep turn is within the performance capability of the aircraft, the convergence of the high-g trim algorithm has been rapid (approximately quadratic), comparable to that for normal 1-g flight.

SMALL-DISTURBANCE EQUATIONS OF MOTION OF AIRCRAFT IN STEADY, HELICAL TURNS

With the trim computation greatly simplified (as discussed in the preceding sections), we may now proceed to compute the small-disturbance equations of motion of an aircraft in a steady, helical turn, using formulas developed in this section. To provide broader applications, some generality will be retained in the following development. Thus, the steady turns to be considered will be both coordinated and uncoordinated, and sideslip will be assumed to be present in those steady turns. To simplify the algebra somewhat, two sets of assumptions will be used:

1. The product of inertia, I_{xy} and I_{yz}, is assumed to be zero

2. The aerodynamic derivatives due to angular acceleration $\dot{p}$, $\dot{q}$, $\dot{r}$ and control-surface deflection rate $\dot{\delta}_a$, $\dot{\delta}_c$, $\dot{\delta}_e$, $\dot{\delta}_p$ are zero

The first assumption is valid for fixed-wing aircraft, though only a good approximation for the single-main-rotor helicopter. The second assumption is made because of a general lack of data for those derivatives; this assumption can thus be relaxed readily when data become available.

The small-disturbance equations of motion are obtained first by applying the perturbation-operation on the Euler equations in general body-axes system (whose steady-state equations for a coordinated or uncoordinated turn are given in eq. (1)) and on the kinematic equations relating the time rate of change of pitch and roll attitudes to the angular rates about the body-axes system, namely,

$$\left.\begin{aligned} \dot{\Theta} &= q \cos \Phi - r \sin \Phi \\ \dot{\Phi} &= p + q \sin \Phi \tan \Theta + r \cos \Phi \tan \Theta \end{aligned}\right\} \tag{13}$$

then imposing the constraints that the perturbations (or the small disturbances) are from a steady turn, that is,

$$\left.\begin{aligned} \dot{\Theta}_o &= q_o \cos \Phi_o - r_o \sin \Phi_o = 0 \\ \dot{\Phi}_o &= p_o + q_o \sin \Phi_o \tan \Theta_o + r_o \cos \Phi_o \tan \Theta_o = 0 \\ \dot{\Psi}_o &= (q_o \sin \Phi_o + r_o \cos \Phi_o) \sec \Theta_o = \text{const.} \end{aligned}\right\} \tag{14}$$

In equation (14), as well as in those that follow, the subscript o signifies the value at the steady flight conditions. The result of the small-disturbance equations, in vector-matrix form, is as follows:

$$\dot{\underline{x}} = F\underline{x} + G\underline{u} \tag{15}$$

where the state vector $\underline{x}$ and control vector $\underline{u}$ are, respectively, the perturbed aircraft motion variables and control surfaces, that is,

$$\underline{x} = (\delta u, \delta w, \delta q, \delta\Theta; \delta v, \delta p, \delta\Phi, \delta r)^T$$

$$\underline{u} = (\tilde{\delta}_e, \tilde{\delta}_c, \tilde{\delta}_a, \tilde{\delta}_p)^T$$

and $\delta u = u - u_o$, $\delta w = w - w_o$, $\tilde{\delta}_e = \delta_e - \delta_{e_o}$, etc. The stability matrix F and the control-effective matrix G are given, respectively, by

$$\left.\begin{aligned} F &= I_E^{-1} A_E \\ G &= I_E^{-1} B_E \end{aligned}\right\} \tag{16}$$

The matrices I_E, A_E, and B_E are given in table 3. The representation of the aerodynamic forces and moments includes complete cross-couplings between the longitudinal and lateral-directional degrees of freedom, and acceleration derivatives. For example, the X force is represented by

$$X = X_o + \sum X_i \delta_i + \text{high-order terms} \tag{17}$$

where $i = u, v, w; p, q, r; \delta_a, \delta_c, \delta_e, \delta_p; \dot{u}, \dot{v}, \dot{w}$. The representation for Y, Z, L, M, and N are similar.

An example showing the stability and control matrices F and G, which includes seven major acceleration derivatives, $Z_{\dot{W}}$, $M_{\dot{W}}$, $L_{\dot{W}}$, $N_{\dot{W}}$, $Y_{\dot{V}}$, $L_{\dot{V}}$, and $N_{\dot{V}}$, is given in table 4. Notice that the structure of the stability matrix F is of the form

$$F = \left[\begin{array}{c|c} \text{Longitudinal} & \begin{array}{c}\text{Couplings of L-D}\\ \text{to longitudinal}\end{array} \\ \hline \begin{array}{c}\text{Couplings of longi-}\\ \text{tudinal to L-D}\end{array} & \begin{array}{c}\text{Lateral-directional}\\ \text{(L-D)}\end{array} \end{array}\right] \tag{18}$$

Notice also that all the kinematic and inertia couplings are present, in addition to the aerodynamic couplings mentioned earlier. With the absence of the acceleration derivatives, the stability and control derivative matrices reduce to a simpler form, as shown in table 5.

For fixed-wing applications, it is sometimes convenient to express the motion of the aircraft in terms of nonorthogonal variables V, α, and β instead of the orthogonal components of the airspeed, u, v, and w. With respect to the new state vector $\underline{y} = (\delta V, \delta\alpha, \delta q, \delta\Theta; \delta\beta, \delta p, \delta\Phi, \delta r)^T$, the stability and control matrices F_y and G_y can be obtained simply by a similarity transformation, that is, $F_y = JFJ^{-1}$, $G_y = JG$, where J is the Jacobian that relates $\underline{x}$ to $\underline{y}$, namely, $\underline{y} = J\underline{x}$.

Some comments pertinent to the earlier development of the small-disturbance equations of motion of the aircraft about steady flight with angular velocity may be of benefit here to provide a historical perspective. In 1938, Frazer et al. (ref. 12) gave an exact expression for the stability matrix F referred to the principal axes (i.e., $I_{xy} = I_{yz} = I_{xz} = 0$) without consideration of any acceleration derivatives. Their formulation is remarkable; they cast the stability matrix in a first-order form such as that employed in this paper, a standard format used in "modern" system theory, thereby converting the aircraft dynamics into an algebraic eigenvalue problem. Abzug (ref. 13) and Thedander (ref. 14) later, in their papers of 1954 and 1965, published an approximate form similar to that of Frazer et al. They referred to the stability axes and expressed the equations in terms of Laplace transform variable — a common practice in linear analyses in the 1940s and 1950s. Our intentions here have been (1) to develop exact equations in general body axes consistent with the expressed assumptions; (2) to avoid possible erroneous conclusions from use of approximate equations; (3) to take into account available data, such as acceleration derivatives, that result from recent developments in experimental and theoretical work related to high-angle-of-attack flight (refs. 15-17); and (4) to cast them in a format to which efficient software packages developed in system theory in the 1960s and 1970s can be adopted for analysis.

APPLICATIONS

The trim algorithm and the algorithm for computing the small-disturbance equations of motion developed in the preceding sections for a general steady, helical turn were implemented for a generic nonlinear real-time simulation model (refs. 18, 19), which was configured to simulate a hingeless-rotor helicopter — representative of a BO-105C (ref. 20); see figure 1. The static (trim) and dynamic characteristics of this simulated helicopter in steep turns were investigated over a range of airspeeds, flightpath angles, and load factors.

Table 6 shows an example of some sample static characteristics of the simulated hingeless-rotor helicopter in coordinated right and left turns. A range of flightpath angles (up to $\pm 20°$) and load factors (up to 2 g) at an airspeed of 60 knots was shown in the table. In general, in a coordinated turn the sideslip β increases with increasing load factor, though somewhat differently in left and right turns. The flightpath angle γ (and the airspeed) also has significant influence on sideslip. The sideslip tends to increase as the flightpath angle increases (and it decreases as the airspeed increases). As more clearly shown in figure 2, the magnitude of the trim pitch attitude Θ of the aircraft also increases as the load factor increases. In coordinated right turns, Θ tends to increase in the nose-up sense; in coordinated

left turns, however, the trim pitch attitude becomes increasingly nose-down as the load factor increases.

The effect of being out of coordination in a steady turn on the sideslip and the aircraft trim pitch attitude is shown in figure 2. For both right and left turns, sideslip increases as n_y becomes increasingly negative (namely, the ball in the turn-and-bank indicator moving increasingly toward right) and decreases as it becomes more positive. For negative n_y, the trim pitch attitude tends to be more nose-up in right turns and more nose-down in left turns. Therefore, to reduce extreme trim pitch attitude and sideslip for this aircraft, it should allow the ball in the turn-and-bank indicator to stay slightly off to the left (rather than at the center or off to the right).

Figures 3 through 5 show the effect of being out of coordination on the relationship between sideslip and trim roll attitude in steady right and left turns for three flightpath angles (γ = 0°, 10°, and -10°) at an airspeed of 60 knots. Because of the sideslip, the trim roll attitude is asymmetrical with respect to the turn direction. The asymmetry becomes more severe when the turn is uncoordinated, especially in a climbing or descending turn.

The stability and control derivative matrices F and G of the same hingeless-rotor helicopter in coordinated and uncoordinated straight-and-level flight and in 2-g level turns, both right and left, are shown in tables 7(a) through 7(i), all at airspeeds of 60 knots. Substantial changes in stability and control derivatives are evident from these tables, as the normal load factor increases from straight and level flight to a 2-g level turn. These changes are due to aerodynamics, kinematics, and inertia. For example, because of aerodynamic effects of the rotor system, the control sensitivity and damping, notably in the pitch and roll axes, increase as the load factor increases (M_{δ_e} = 1.022 rad/sec^2/in., M_q = -3.993/sec, L'_{δ_a} = 2.366 rad/sec^2/in., and L'_p = -9.576/sec at 1-g straight-and-level coordinated flight to M_{δ_e} = 1.173, M_q = -4.528, L'_{δ_a} = 2.742, and L'_p = -11.168 at 2-g level, coordinated right turn). Kinematic effects as reflected in the increase in sideslip, a result of increased load factor and being out of coordination in steady turns as described earlier, can also be seen from these tables (e.g., the last element in the first row of the matrix F). The effects of the turn direction on some elements of the stability matrix F can also be seen in table 7 by comparing elements for the right and left turns. These effects include, for example, kinematic and inertia contributions owing to the asymmetry in roll attitude Φ, yaw rate r, and the rate of turn $\dot{\Psi}$. Linear analyses using some of these and other derivative matrices have been performed recently (ref. 11) to investigate the flight dynamics and control characteristics of rotorcraft in steep, high-g turns.

The developed trim algorithm and the algorithm for computing the small-disturbance equations of motion for a general steep turn have also been incorporated into a nonlinear, full-flight envelope simulation model for a tilt-rotor aircraft (ref. 21) to examine the high-g flight dynamics for all its three operating modes: the airplane mode, the conversion mode, and the helicopter mode. The results are being documented. Applications of the algorithms are also being made to investigate the high-g flight dynamics of a current generation military utility helicopter, which has an articulated main rotor (ref. 22).

Future applications of the computational algorithms developed herein to fixed-wing aircraft could be of significant promise. For example, they can be adapted, in

a manner similar to that in which they were adapted to rotorcraft (described above), to high-performance fighter aircraft to examine their stall and departure characteristics (refs. 23-26), to multiengine transport aircraft to assess flight dynamics and control characteristics in engine-out asymmetrical flight, and to general aviation aircraft to identify potential problems in steep turns at low speeds (ref. 1).

CONCLUDING REMARKS

Efficient computational algorithms have been developed that permit a systematic investigation of the statics (trim) and dynamics of aircraft in steady coordinated or uncoordinated steep-turning flight. The calculation of aircraft trim states and control positions has been greatly simplified by decoupling the set of 11 equations governing a general steady, helical turn. This was done by solving explicitly for the aircraft attitudes and body-axis angular rates in terms of all other flight parameters involving a steep turn.

The exact small-disturbance equations of motion of the aircraft in general steady turns have also been developed to expedite the study of flight dynamics of rotary-wing and fixed-wing aircraft in extreme conditions. These equations have been given with respect to general body axes and with aerodynamic acceleration derivatives included. They have been cast in the first-order, vector-matrix format, and are thus compatible with many efficient software packages developed in modern system theory.

Applications of those algorithms to a variety of rotorcraft have been made. In particular, some results pertaining to a simulated hingeless-rotor helicopter have been discussed in the report. Applications to fixed-wing aircraft, including high-performance fighter aircraft, multiengine transport aircraft, and general aviation aircraft should be of potential benefit.

APPENDIX

DERIVATION OF THE EXPLICIT KINEMATIC RELATIONSHIPS FOR AIRCRAFT ANGULAR RATES AND ATTITUDES IN A STEADY HELICAL TURN

In this appendix the aircraft attitudes Θ and Φ and body-axis angular rates p, q, and r in a steady uncoordinated helical turn will be solved explicitly in terms of the turn parameters V, γ, and $\dot{\Psi}$; body-axis specific side force n_y; angle of attack α; and angle of sideslip β. This development, therefore, amounts to an extension of the previous work as described in reference 9 for coordinated helical turns. The equations governing a steady, uncoordinated, helical turn with a specific sideforce $n_y \triangleq Y/mg$ are as follows:

$$\frac{X}{mg} - \sin\Theta - \tan\phi_1(\sin\alpha\cos\beta\cos\Theta\sin\Phi - \sin\beta\cos\Theta\cos\Phi) = 0 \qquad \text{(A1a)}$$

$$\frac{Y}{mg} + \cos\Theta\sin\Phi - \tan\phi_1\cos\beta(\cos\alpha\cos\Theta\cos\Phi + \sin\alpha\sin\Theta) = 0 \qquad \text{(A1b)}$$

$$\frac{Z}{mg} + \cos\Theta\cos\Phi + \tan\phi_1(\sin\beta\sin\Theta + \cos\alpha\cos\beta\cos\Theta\sin\Phi) = 0 \qquad \text{(A1c)}$$

$$L + I_{yz}(q^2 - r^2) + I_{xz}pq - I_{xy}rp + (I_y - I_z)qr = 0 \qquad \text{(A1d)}$$

$$M + I_{xz}(r^2 - p^2) + I_{xy}qr - I_{yz}pq + (I_z - I_x)rp = 0 \qquad \text{(A1e)}$$

$$N + I_{xy}(p^2 - q^2) + I_{yz}rp - I_{xz}qr + (I_x - I_y)pq = 0 \qquad \text{(A1f)}$$

$$\sin\gamma = \cos\alpha\cos\beta\sin\Theta - (\sin\beta\sin\Phi + \sin\alpha\cos\beta\cos\Phi)\cos\Theta \qquad \text{(A2a)}$$

$$p = -\dot{\Psi}\sin\Theta \qquad \text{(A2b)}$$

$$q = \dot{\Psi}\cos\Theta\sin\Phi \qquad \text{(A2c)}$$

$$r = \dot{\Psi}\cos\Theta\cos\Phi \qquad \text{(A2d)}$$

Multiplying equation (A1b) by $\dot{\Psi}$ and substituting equations (A2b) through (A2d) into the resulting equation yields

$$q = \tan\phi_1\cos\beta(r\cos\alpha - p\sin\alpha) - \dot{\Psi}n_y \qquad \text{(A3)}$$

Using the same procedure, equation (A2a) becomes

$$q\tan\beta = -\frac{\dot{\Psi}\sin\gamma}{\cos\beta} - (p\cos\alpha + r\sin\alpha) \qquad \text{(A4)}$$

Let p' and r' be defined by

$$\begin{bmatrix} p' \\ r' \end{bmatrix} = \begin{bmatrix} \cos\alpha & \sin\alpha \\ -\sin\alpha & \cos\alpha \end{bmatrix} \begin{bmatrix} p \\ r \end{bmatrix} \tag{A5}$$

Then equations (A3) and (A4) become (A6) and (A7), respectively:

$$r' = \frac{q + \dot{\Psi} n_y}{\tan\phi_1 \cos\beta} \tag{A6}$$

$$p' = -\frac{\dot{\Psi} \sin\gamma}{\cos\beta} - q \tan\beta \tag{A7}$$

Using the identity $\dot{\Psi}^2 = p^2 + q^2 + r^2 = p'^2 + q^2 + r'^2$, the pitch rate q can be solved to yield

$$q = \dot{\Psi} \sin^2\phi_1 \left\{ -(\sin\gamma \sin\beta + n_y \operatorname{cotan}^2\phi_1) \pm \left[(\sin\gamma \sin\beta + n_y \operatorname{cotan}^2\phi_1)^2 - \frac{1}{\sin^2\phi_1} (\sin^2\gamma - \cos^2\beta + n_y^2 \operatorname{cotan}^2\phi_1) \right]^{1/2} \right\} \tag{A8}$$

$$q \geq 0$$

With q thus obtained, p and r can be readily computed, using (A6), (A7), and the following equations:

$$p = p' \cos\alpha - r' \sin\alpha \tag{A9}$$

$$r = p' \sin\alpha + r' \cos\alpha \tag{A10}$$

Once again using equations (A2b)-(A2d), the pitch and roll attitudes can be computed, using

$$\Theta = \sin^{-1}\left(\frac{-p}{\dot{\Psi}}\right) \tag{A11}$$

$$\Phi = \tan^{-1}\left(\frac{q}{r}\right) \tag{A12}$$

For a coordinated or uncoordinated straight flight, $\dot{\Psi}$, as well as the body-axis angular rates p, q, and r, are all identically zero. Therefore, the computational formulas (A11) and (A12) for the aircraft pitch and roll attitudes become indefinite, and an alternative set of formulas is required. From equations (A1a)-(A1c), we have

$$\sin\Phi = -n_y/\cos\Theta \tag{A13}$$

$$\cos\Theta \cos\Phi = (1 - n_y^2 - \sin^2\Theta)^{1/2} \tag{A14}$$

Using the above two equations and equation (A2a), we obtain

$$\sin \Theta = \frac{\cos \alpha(\sin \gamma - n_y \sin \beta) + \sin \alpha[\cos^2\beta - \sin^2\gamma + n_y(2 \sin \beta \sin \gamma - n_y)]^{1/2}}{\cos \beta} \tag{A15}$$

Equations (A15) and (A13) are the desired formulas for computing the aircraft pitch and roll attitudes for general uncoordinated, steady, straight flight.

REFERENCES

1. Anderson, Seth B.: A Historical Overview of Stall/Spin Characteristics of General Aviation Aircraft. J. Aircraft, vol. 16, July 1979.

2. Tail Rotor Stall. U.S. Army Aviation Digest, Nov. 1978, pp. 43-45.

3. Etkin, B.: Dynamics of Atmospheric Flight. John Wiley & Sons, Inc., New York, 1972.

4. Seckel, E.: Stability and Control of Airplanes and Helicopters. Academic Press, New York, 1964.

5. General Requirements for Helicopter Flying and Ground Handling Qualities. Specification MIL-H-8501A, Sept. 1961.

6. V/STOL Handling. Part I. Criteria and Discussion. AGARD Report 577, June 1973.

7. Flying Qualities of Piloted V/STOL Aircraft. Specification MIL-F-83300, Dec. 31, 1970.

8. Flying Qualities of Piloted Airplanes. Specification MIL-F-8785B(ASG), 7 Aug. 1969.

9. Chen, R. T. N.; and Jeske, J. A.: Kinematic Properties of the Helicopter in Coordinated Turns. NASA TP-1773, 1981.

10. Chen, R. T. N.: Kinematic Properties of Rotary-Wing and Fixed-Wing Aircraft in Steady Coordinated High-g Turns. AIAA Paper 81-1855, Aug. 1981.

11. Chen, R. T. N.: Flight Dynamics of Rotorcraft in Steep High-g Turns. AIAA Paper 82-1345, Aug. 1982.

12. Frazer, R. A.; Duncan, W. J.; and Collar, A. R.: Elementary Matrices. Cambridge University Press, 1938, p. 287.

13. Abzug, M. J.: Effects of Certain Steady Motions on Small-Disturbance Airplane Dynamics. J. Aeronaut. Sci., Nov. 1954, pp. 749-752.

14. Thedander, J. A.: Aircraft Motion Analysis. Report FDL-TDR-64-70, Mar. 1965.

15. Orlik-Ruckemann, K. J.: Aerodynamic Coupling between Lateral and Longitudinal Degrees of Freedom. AIAA J., vol. 15, no. 12, Dec. 1977, pp. 1792-1799.

16. Coe, P. L., Jr.; Graham, A. B.; and Chambers, J. R.: Summary of Information on Low-Speed Lateral Directional Derivatives Due to Rate of Change of Sideslip. NASA TN D-7972, 1975.

17. Schiff, L. B.; Tobak, M.; and Malcolm, G. N.: Mathematical Modeling of the Aerodynamics of High-Angle-of-Attack Maneuvers. AIAA Paper 80-1583-CP, Aug. 1980.

18. Chen, R. T. N.: A Simplified Rotor System Mathematical Model for Piloted Flight Dynamics Simulation. NASA TM-78575, 1979.

19. Talbot, P. D.; Tinling, B. E.; Decker, W. A.; and Chen, R. T. N.: A Mathematical Model of a Single Main Rotor Helicopter for Piloted Simulation. NASA TM-84281, Sept. 1982.

20. Heffley, R. K.; et al.: A Compilation and Analysis of Helicopter Handling Qualities Data. Vol. I. NASA CR-3144, 1979.

21. Harendra, P. B.; et al.: V/STOL Tilt Rotor Study. Vol. V. A Mathematical Model for Real Time Flight Simulation of the Bell Model 301 Tilt Rotor Research Aircraft. NASA CR-114614, 1973.

22. Howlett, J. J.: UH-60A Black Hawk Engineering Simulation Program. Vol. I. Mathematical Model. NASA CR-166309, 1981.

23. Chen, R. T. N.; Newell, F. D.; and Schelhorn, A. E.: Development and Evaluation of an Automatic Departure Prevention System and Stall Inhibitor for Fighter Aircraft. AFFDL-TR-73-29, Apr. 1973.

24. Butler, R. W.; and Langham, T. F.: Aircraft Motion Sensitivity to Variations in Dynamic Stability Parameters. AGARD CP-235, Paper 35, 1978.

25. Langham, T. F.: Aircraft Motion Sensitivity to Dynamic Stability Derivatives. AEDC-TR-79-11, Jan. 1980.

26. Orlik-Ruckemann, K. J.: Sensitivity of Aircraft Motion to Cross-Coupling and Acceleration Derivatives. Dynamic Stability Parameters, AGARD Lecture Series Preprint No. 114, Feb. 1981, pp. 15-1 to 15-13.

TABLE 1.- EQUATIONS GOVERNING AN AIRCRAFT IN A STEADY COORDINATED HELICAL TURN

$$\frac{X}{mg} - \sin\Theta - \tan\phi_1(\sin\alpha\cos\beta\cos\Theta\sin\Phi - \sin\beta\cos\Theta\cos\Phi) = 0 \qquad (1a)$$

$$\frac{Y}{mg} + \cos\Theta\sin\Phi - \tan\phi_1\cos\beta(\cos\alpha\cos\Theta\cos\Phi + \sin\alpha\sin\Theta) = 0 \qquad (1b)$$

$$\frac{Z}{mg} + \cos\Theta\cos\Phi + \tan\phi_1(\sin\beta\sin\Theta + \cos\alpha\cos\beta\cos\Theta\sin\Phi) = 0 \qquad (1c)$$

$$L + I_{yz}(q^2 - r^2) + I_{xz}pq - I_{xy}rp + (I_y - I_z)qr = 0 \qquad (1d)$$

$$M + I_{xz}(r^2 - p^2) + I_{xy}qr - I_{yz}pq + (I_z - I_x)rp = 0 \qquad (1e)$$

$$N + I_{xy}(p^2 - q^2) + I_{yz}rp - I_{xz}qr + (I_x - I_y)pq = 0 \qquad (1f)$$

$$\sin\Phi = \tan\phi_1(\cos\alpha\cos\Phi + \sin\alpha\tan\Theta)\cos\beta \qquad (2a)'$$

$$\sin\gamma = \cos\alpha\cos\beta\sin\Theta - (\sin\beta\sin\Phi + \sin\alpha\cos\beta\cos\Phi)\cos\Theta \qquad (2b)$$

$$p = -\dot{\Psi}\sin\Theta \qquad (2c)$$

$$q = \dot{\Psi}\cos\Theta\sin\Phi \qquad (2d)$$

$$r = \dot{\Psi}\cos\Theta\cos\Phi \qquad (2e)$$

TABLE 2.- EQUATIONS GOVERNING AN AIRCRAFT IN A STEADY UNCOORDINATED STEEP TURN

Steady-state Euler equations

$$n_x - \sin\Theta - \tan\phi_1(\sin\alpha\cos\beta\cos\Theta\sin\Phi - \sin\beta\cos\Theta\cos\Phi) = 0$$

$$n_y + \cos\Theta\sin\Phi - \tan\phi_1\cos\beta(\cos\alpha\cos\Theta\cos\Phi + \sin\alpha\sin\Theta) = 0$$

$$n_z + \cos\Theta\cos\Phi + \tan\phi_1(\sin\beta\sin\Theta + \cos\alpha\cos\beta\cos\Theta\sin\Phi) = 0$$

$$L + I_{yz}(q^2 - r^2) + I_{xz}pq - I_{xy}rp + (I_y - I_z)qr = 0$$

$$M + I_{xz}(r^2 - p^2) + I_{xy}qr - I_{yz}pq + (I_z - I_x)rp = 0$$

$$N + I_{xy}(p^2 - q^2) + I_{yz}rp - I_{xz}qr + (I_x - I_y)pq = 0$$

$$\phi_1 = \tan^{-1}\left(\frac{\dot{\Psi}V}{g}\right)$$

$$= \pm\tan^{-1}\left[\frac{(n^2 - 1)^{1/2}}{\cos\gamma}\right], \quad + \text{right turn; - left turn}$$

$$n^2 = n_x^2 + n_y^2 + n_z^2$$

Kinematic relationships

$$q = \dot{\Psi}\sin^2\phi_1\left\{-(\sin\gamma\sin\beta + n_y\,\text{cotan}^2\phi_1) \pm \left[(\sin\gamma\sin\beta + n_y\,\text{cotan}^2\phi_1)^2 - \frac{1}{\sin^2\phi_1}(\sin^2\gamma - \cos^2\beta + n_y^2\,\text{cotan}^2\phi_1)\right]^{1/2}\right\}$$

$$q \geq 0$$

$$r' = \frac{q + \dot{\Psi}n_y}{\tan\phi_1\cos\beta}$$

$$p' = -\frac{\dot{\Psi}\sin\gamma}{\cos\beta} - q\tan\beta$$

$$p = p'\cos\alpha - r'\sin\alpha$$

$$r = p'\sin\alpha + r'\cos\alpha$$

$$\Theta = \sin^{-1}(-p/\dot{\Psi})$$

$$\Phi = \tan^{-1}(q/r)$$

TABLE 3.- MATRICES I_E, A_E, AND B_E

$$I_E = \begin{bmatrix} m - X_{\dot{u}} & -X_{\dot{w}} & 0 & 0 & -X_{\dot{v}} & 0 & 0 & 0 \\ -Z_{\dot{u}} & m - Z_{\dot{w}} & 0 & 0 & -Z_{\dot{v}} & 0 & 0 & 0 \\ -M_{\dot{u}} & -M_{\dot{w}} & I_y & 0 & -M_{\dot{v}} & 0 & 0 & 0 \\ 0 & 0 & 0 & 1 & 0 & 0 & 0 & 0 \\ -Y_{\dot{u}} & -Y_{\dot{w}} & 0 & 0 & m - Y_{\dot{v}} & 0 & 0 & 0 \\ -L_{\dot{u}} & -L_{\dot{w}} & 0 & 0 & -L_{\dot{v}} & I_x & 0 & -I_{xz} \\ 0 & 0 & 0 & 0 & 0 & 0 & 1 & 0 \\ -N_{\dot{u}} & -N_{\dot{w}} & 0 & 0 & -N_{\dot{v}} & -I_{xz} & 0 & I_z \end{bmatrix}$$

$$B_E = \begin{bmatrix} X_{\delta_e} & X_{\delta_c} & X_{\delta_a} & X_{\delta_p} \\ Z_{\delta_e} & Z_{\delta_c} & Z_{\delta_a} & Z_{\delta_p} \\ M_{\delta_e} & M_{\delta_c} & M_{\delta_a} & M_{\delta_p} \\ 0 & 0 & 0 & 0 \\ Y_{\delta_e} & Y_{\delta_c} & Y_{\delta_a} & Y_{\delta_p} \\ L_{\delta_e} & L_{\delta_c} & L_{\delta_a} & L_{\delta_p} \\ 0 & 0 & 0 & 0 \\ N_{\delta_e} & N_{\delta_c} & N_{\delta_a} & N_{\delta_p} \end{bmatrix}$$

TABLE 3.- Concluded.

$$A_E = \begin{bmatrix}
X_u & X_w - mq_0 & X_q - mw_0 & -mg\cos\Theta_0 & X_v + mr_0 & X_p & 0 & X_r + mv_0 \\
Z_u + mq_0 & Z_w & Z_q + mu_0 & -mg\cos\Phi_0\sin\Theta_0 & Z_v - mp_0 & Z_p - mv_0 & -mg\sin\Phi_0\cos\Theta_0 & Z_r \\
M_u & M_w & M_q & 0 & M_v & \begin{matrix} M_p - 2p_0 I_{xz} \\ -r_0(I_x - I_z) \end{matrix} & 0 & \begin{matrix} M_r + 2r_0 I_{xz} \\ -p_0(I_x - I_z) \end{matrix} \\
0 & 0 & \cos\Phi_0 & 0 & 0 & 0 & -\dot{\Psi}_0\cos\Theta_0 & -\sin\phi_0 \\
Y_u - mr_0 & Y_w + mp_0 & Y_q & -mg\sin\Phi_0\sin\Theta_0 & Y_v & Y_p + mw_0 & mg\cos\Phi_0\cos\Theta_0 & Y_r - mu_0 \\
L_u & L_w & \begin{matrix} L_q + p_0 I_{xz} \\ -r_0(I_z - I_y) \end{matrix} & 0 & L_v & L_p + q_0 I_{xz} & 0 & \begin{matrix} L_r - q_0(I_z \\ -I_y) \end{matrix} \\
0 & 0 & \sin\Phi_0\tan\Theta_0 & \dot{\Psi}_0\sec\Theta_0 & 0 & 1 & 0 & \cos\Phi_0\tan\Theta_0 \\
N_u & N_w & \begin{matrix} N_q - r_0 I_{xz} \\ -p_0(I_y - I_x) \end{matrix} & 0 & N_v & \begin{matrix} N_p - q_0(I_y \\ -I_x) \end{matrix} & 0 & N_r - q_0 I_{xz}
\end{bmatrix}$$

TABLE 4.- STABILITY AND CONTROL MATRICES INCLUDING SEVEN MAJOR ACCELERATION DERIVATIVES

$$
F = \begin{bmatrix}
x_u & x_w - q_0 & x_q - w_0 & -g\cos\Theta_0 & x_v + r_0 & x_p & 0 & x_r + v_0 \\
\dfrac{z_u + q_0}{1 - z_{\dot{w}}} & \dfrac{z_w}{1 - z_{\dot{w}}} & \dfrac{z_q + u_0}{1 - z_{\dot{w}}} & \dfrac{-g\cos\Phi_0\sin\Theta_0}{1 - z_{\dot{w}}} & \dfrac{z_v - p_0}{1 - z_{\dot{w}}} & \dfrac{z_p - v_0}{1 - z_{\dot{w}}} & \dfrac{-g\sin\Phi_0\cos\Theta_0}{1 - z_{\dot{w}}} & \dfrac{z_r}{1 - z_{\dot{w}}} \\
m_u + \dfrac{m_{\dot{w}}(z_u + q_0)}{1 - z_{\dot{w}}} & m_w + \dfrac{m_{\dot{w}} z_w}{1 - z_{\dot{w}}} & m_q + \dfrac{m_{\dot{w}}(z_q + u_0)}{1 - z_{\dot{w}}} & \dfrac{-g\, m_{\dot{w}}\cos\Phi_0\sin\Theta_0}{1 - z_{\dot{w}}} & m_v + \dfrac{m_{\dot{w}}(z_v - p_0)}{1 - z_{\dot{w}}} & \begin{matrix} m_p - 2p_0 I_{xz}/I_y \\ + r_0(I_z - I_x)/I_y \\ + m_{\dot{w}}(z_p - v_0)/(1 - z_{\dot{w}}) \end{matrix} & \dfrac{-g\, m_{\dot{w}}\sin\Phi_0\cos\Theta_0}{1 - z_{\dot{w}}} & \begin{matrix} m_r + 2r_0 I_{xz}/I_y \\ + p_0(I_z - I_x)/I_y \\ + m_{\dot{w}} z_r/(1 - z_{\dot{w}}) \end{matrix} \\
0 & 0 & \cos\Phi_0 & 0 & 0 & 0 & -\dot{\Psi}_0\cos\Theta_0 & -\sin\Phi_0 \\
\dfrac{y_u - r_0}{1 - y_{\dot{v}}} & \dfrac{y_w + p_0}{1 - y_{\dot{v}}} & \dfrac{y_q}{1 - y_{\dot{v}}} & \dfrac{-g\sin\Phi_0\sin\Theta_0}{1 - y_{\dot{v}}} & \dfrac{y_v}{1 - y_{\dot{v}}} & \dfrac{y_p + w_0}{1 - y_{\dot{v}}} & \dfrac{g\cos\Phi_0\cos\Theta_0}{1 - y_{\dot{v}}} & \dfrac{y_r - u_0}{1 - y_{\dot{v}}} \\
\begin{matrix} \ell'_u + \dfrac{\ell'_{\dot{v}}(y_u - r_0)}{1 - y_{\dot{v}}} \\ + \dfrac{\ell'_{\dot{w}}(z_u + q_0)}{1 - z_{\dot{w}}} \end{matrix} & \begin{matrix} \ell'_w + \dfrac{\ell'_{\dot{v}}(y_w + p_0)}{1 - y_{\dot{v}}} \\ + \dfrac{\ell'_{\dot{w}} z_w}{1 - z_{\dot{w}}} \end{matrix} & \begin{matrix} \ell'_q + t_1 p_0 - t_2 r_0 \\ + \ell'_{\dot{v}} y_q/(1 - y_{\dot{v}}) \\ + \ell'_{\dot{w}}(z_q + u_0)/(1 - z_{\dot{w}}) \end{matrix} & \begin{matrix} \dfrac{-g\,\ell'_{\dot{v}}\sin\Phi_0\sin\Theta_0}{1 - y_{\dot{v}}} \\ - \dfrac{g\,\ell'_{\dot{w}}\cos\Phi_0\sin\Theta_0}{1 - z_{\dot{w}}} \end{matrix} & \begin{matrix} \ell'_v + \dfrac{\ell'_{\dot{v}} y_v}{1 - y_{\dot{v}}} \\ + \dfrac{\ell'_{\dot{w}}(z_v - p_0)}{1 - z_{\dot{w}}} \end{matrix} & \begin{matrix} \ell'_p + t_1 q_0 + \dfrac{\ell'_{\dot{v}}(y_p + w_0)}{1 - y_{\dot{v}}} \\ + \dfrac{\ell'_{\dot{w}}(z_p - v_0)}{1 - z_{\dot{w}}} \end{matrix} & \begin{matrix} \dfrac{\ell'_{\dot{v}}\, g\cos\Phi_0\cos\Theta_0}{1 - y_{\dot{v}}} \\ - \dfrac{\ell'_{\dot{w}}\, g\sin\Phi_0\cos\Theta_0}{1 - z_{\dot{w}}} \end{matrix} & \begin{matrix} \ell'_r - t_2 q_0 + \dfrac{\ell'_{\dot{v}}(y_r - u_0)}{1 - y_{\dot{v}}} \\ + \dfrac{\ell'_{\dot{w}} z_r}{1 - z_{\dot{w}}} \end{matrix} \\
0 & 0 & \sin\Phi_0\tan\Theta_0 & \dot{\Psi}_0\sec\Theta_0 & 0 & 1 & 0 & \cos\Phi_0\tan\Theta_0 \\
\begin{matrix} n'_u + \dfrac{n'_{\dot{v}}(y_u - r_0)}{1 - y_{\dot{v}}} \\ + \dfrac{n'_{\dot{w}}(z_u + q_0)}{1 - z_{\dot{w}}} \end{matrix} & \begin{matrix} n'_w + \dfrac{n'_{\dot{v}}(y_w + p_0)}{1 - y_{\dot{v}}} \\ + \dfrac{n'_{\dot{w}} z_w}{1 - z_{\dot{w}}} \end{matrix} & \begin{matrix} n'_q - t_1 r_0 - t_3 p_0 \\ + n'_{\dot{v}} y_q/(1 - y_{\dot{v}}) \\ + n'_{\dot{w}}(z_q + u_0)/(1 - z_{\dot{w}}) \end{matrix} & \begin{matrix} \dfrac{-g\, n'_{\dot{v}}\sin\Phi_0\sin\Theta_0}{1 - y_{\dot{v}}} \\ - \dfrac{g\, n'_{\dot{w}}\cos\Phi_0\sin\Theta_0}{1 - z_{\dot{w}}} \end{matrix} & \begin{matrix} n'_v + \dfrac{n'_{\dot{v}} y_v}{1 - y_{\dot{v}}} \\ + \dfrac{n'_{\dot{w}}(z_v - p_0)}{1 - z_{\dot{w}}} \end{matrix} & \begin{matrix} n'_p - t_3 q_0 + \dfrac{n'_{\dot{v}}(y_p + w_0)}{1 - y_{\dot{v}}} \\ + \dfrac{n'_{\dot{w}}(z_p - v_0)}{1 - z_{\dot{w}}} \end{matrix} & \begin{matrix} \dfrac{n'_{\dot{v}}\, g\cos\Phi_0\cos\Theta_0}{1 - y_{\dot{v}}} \\ - \dfrac{n'_{\dot{w}}\, g\sin\Phi_0\cos\Theta_0}{1 - z_{\dot{w}}} \end{matrix} & \begin{matrix} n'_r - t_1 q_0 + \dfrac{n'_{\dot{v}}(y_r - u_0)}{1 - y_{\dot{v}}} \\ + \dfrac{n'_{\dot{w}} z_r}{1 - z_{\dot{w}}} \end{matrix}
\end{bmatrix}
$$

TABLE 4.- Concluded.

$$
G = \begin{bmatrix}
x_{\delta_e} & x_{\delta_c} & x_{\delta_a} & x_{\delta_p} \\
\dfrac{z_{\delta_e}}{1 - z_{\dot{w}}} & \dfrac{z_{\delta_c}}{1 - z_{\dot{w}}} & \dfrac{z_{\delta_a}}{1 - z_{\dot{w}}} & \dfrac{z_{\delta_p}}{1 - z_{\dot{w}}} \\
m_{\delta_e} + \dfrac{m_{\dot{w}} z_{\delta_e}}{1 - z_{\dot{w}}} & m_{\delta_c} + \dfrac{m_{\dot{w}} z_{\delta_c}}{1 - z_{\dot{w}}} & m_{\delta_a} + \dfrac{m_{\dot{w}} z_{\delta_a}}{1 - z_{\dot{w}}} & m_{\delta_p} + \dfrac{m_{\dot{w}} z_{\delta_p}}{1 - z_{\dot{w}}} \\
0 & 0 & 0 & 0 \\
\dfrac{y_{\delta_e}}{1 - y_{\dot{v}}} & \dfrac{y_{\delta_c}}{1 - y_{\dot{v}}} & \dfrac{y_{\delta_a}}{1 - y_{\dot{v}}} & \dfrac{y_{\delta_p}}{1 - y_{\dot{v}}} \\
\ell'_{\delta_e} + \dfrac{\ell'_{\dot{v}} y_{\delta_e}}{1 - y_{\dot{v}}} + \dfrac{\ell'_{\dot{w}} z_{\delta_e}}{1 - z_{\dot{w}}} & \ell'_{\delta_c} + \dfrac{\ell'_{\dot{v}} y_{\delta_c}}{1 - y_{\dot{v}}} + \dfrac{\ell'_{\dot{w}} z_{\delta_c}}{1 - z_{\dot{w}}} & \ell'_{\delta_a} + \dfrac{\ell'_{\dot{v}} y_{\delta_a}}{1 - y_{\dot{v}}} + \dfrac{\ell'_{\dot{w}} z_{\delta_a}}{1 - z_{\dot{w}}} & \ell'_{\delta_p} + \dfrac{\ell'_{\dot{v}} y_{\delta_p}}{1 - y_{\dot{v}}} + \dfrac{\ell'_{\dot{w}} z_{\delta_p}}{1 - z_{\dot{w}}} \\
0 & 0 & 0 & 0 \\
n'_{\delta_e} + \dfrac{n'_{\dot{v}} y_{\delta_e}}{1 - y_{\dot{v}}} + \dfrac{n'_{\dot{w}} z_{\delta_e}}{1 - z_{\dot{w}}} & n'_{\delta_c} + \dfrac{n'_{\dot{v}} y_{\delta_c}}{1 - y_{\dot{v}}} + \dfrac{n'_{\dot{w}} z_{\delta_c}}{1 - z_{\dot{w}}} & n'_{\delta_a} + \dfrac{n'_{\dot{v}} y_{\delta_a}}{1 - y_{\dot{v}}} + \dfrac{n'_{\dot{w}} z_{\delta_a}}{1 - z_{\dot{w}}} & n'_{\delta_p} + \dfrac{n'_{\dot{v}} y_{\delta_p}}{1 - y_{\dot{v}}} + \dfrac{n'_{\dot{w}} z_{\delta_p}}{1 - z_{\dot{w}}}
\end{bmatrix}
$$

where

$$x_i = \frac{X_i}{m} \; ; \quad y_i = \frac{Y_i}{m} \; ; \quad z_i = \frac{Z_i}{m}$$

$$m_i = \frac{M_i}{I_y}$$

$$\ell'_i = \frac{I_z}{I_x I_z - I_{xz}^2} L_i + \frac{I_{xz}}{I_x I_z - I_{xz}^2} N_i$$

$$n'_i = \frac{I_{xz}}{I_x I_z - I_{xz}^2} L_i + \frac{I_x}{I_x I_z - I_{xz}^2} N_i$$

$$t_1 = \frac{I_{xz}(I_z + I_x - I_y)}{I_x I_z - I_{xz}^2} \; ; \quad t_2 = \frac{I_z(I_z - I_y) + I_{xz}^2}{I_x I_z - I_{xz}^2} \; ; \quad t_3 = \frac{I_x(I_y - I_x) - I_{xz}^2}{I_x I_z - I_{xz}^2}$$

TABLE 5.- SMALL-PERTURBATION EQUATIONS OF MOTION OF AIRCRAFT FROM STEADY TURNING FLIGHT
(WITH ACCELERATION DERIVATIVES NEGLECTED)

$$\dot{\underline{x}} = F\underline{x} + G\underline{u}$$

$$\underline{x} \triangleq (\delta u,\ \delta w,\ \delta q,\ \delta\Theta;\ \delta v,\ \delta p,\ \delta\Phi,\ \delta r)^T$$

$$\underline{u} \triangleq (\Delta\delta_e,\ \Delta\delta_c,\ \Delta\delta_a,\ \Delta\delta_p)^T$$

$$F = \begin{bmatrix}
x_u & x_w - q_0 & x_q - w_0 & -g\cos\Theta_0 & x_v + r_0 & x_p & 0 & x_r + v_0 \\
z_u + q_0 & z_w & z_q + u_0 & -g\cos\Phi_0\sin\Theta_0 & z_v - p_0 & z_p - v_0 & -g\sin\Phi_0\cos\Theta_0 & z_r \\
m_u & m_w & m_q & 0 & m_v & \begin{matrix} m_p - 2p_0\dfrac{I_{xz}}{I_y} \\ -r_0\dfrac{(I_x - I_z)}{I_y} \end{matrix} & 0 & \begin{matrix} m_r + 2r_0\dfrac{I_{xz}}{I_y} \\ -p_0\dfrac{(I_x - I_z)}{I_y} \end{matrix} \\
0 & 0 & \cos\Phi_0 & 0 & 0 & 0 & -\dot{\Psi}_0\cos\Theta_0 & -\sin\Phi_0 \\
y_u - r_0 & y_w + p_0 & y_q & -g\sin\Phi_0\sin\Theta_0 & y_v & y_p + w_0 & g\cos\Phi_0\cos\Theta_0 & y_r - u_0 \\
\ell'_u & \ell'_w & \ell'_q + t_1p_0 - t_2r_0 & 0 & \ell'_v & \ell'_p + t_1q_0 & 0 & \ell'_r - t_2q_0 \\
0 & 0 & \sin\Phi_0\tan\Theta_0 & \dot{\Psi}_0\sec\Theta_0 & 0 & 1 & 0 & \cos\Phi_0\tan\Theta_0 \\
n'_u & n'_w & n'_q - t_3p_0 - t_1r_0 & 0 & n'_v & n'_p - t_3q_0 & 0 & n'_r - t_1q_0
\end{bmatrix}$$

TABLE 5.- Concluded.

$$G = \begin{bmatrix} x_{\delta_e} & x_{\delta_c} & x_{\delta_a} & x_{\delta_p} \\ z_{\delta_e} & z_{\delta_c} & z_{\delta_a} & z_{\delta_p} \\ m_{\delta_e} & m_{\delta_c} & m_{\delta_a} & m_{\delta_p} \\ 0 & 0 & 0 & 0 \\ y_{\delta_e} & y_{\delta_c} & y_{\delta_a} & y_{\delta_p} \\ \ell'_{\delta_e} & \ell'_{\delta_c} & \ell'_{\delta_a} & \ell'_{\delta_p} \\ 0 & 0 & 0 & 0 \\ n'_{\delta_e} & n'_{\delta_c} & n'_{\delta_a} & n'_{\delta_p} \end{bmatrix}$$

where

$$\left.\begin{aligned} x_i &= \frac{X_i}{m} \; ; \; y_i = \frac{Y_i}{m} \; ; \; z_i = \frac{Z_i}{m} \\ m_i &= \frac{M_i}{I_y} \end{aligned}\right\} \quad i = u, v, w; p, q, r; \delta_e, \delta_c, \delta_a, \delta_p$$

$$\ell'_i = \frac{I_z}{I_x I_z - I_{xz}^2} L_i + \frac{I_{xz}}{I_x I_z - I_{xz}^2} N_i$$

$$n'_i = \frac{I_{xz}}{I_x I_z - I_{xz}^2} L_i + \frac{I_x}{I_x I_z - I_{xz}^2} N_i$$

$$t_1 = \frac{I_{xz}(I_z + I_x - I_y)}{I_x I_z - I_{xz}^2} \; ; \qquad t_2 = \frac{I_z(I_z - I_y) + I_{xz}^2}{I_x I_z - I_{xz}^2} \; ; \qquad t_3 = \frac{I_x(I_y - I_x) - I_{xz}^2}{I_x I_z - I_{xz}^2}$$

TABLE 6.- TRIM VALUES OF THE HINGELESS-ROTOR HELICOPTER IN COORDINATED TURNING FLIGHT[a]

Turn direction	Normal load factor, g	α, deg	β, deg	Θ, deg	Φ, deg	p, deg/sec	q, deg/sec	r, deg/sec	$\dot{\Psi}$, deg/sec	Turn radius, ft
$\gamma = 0°$										
--	1	0.46	6.53	0.46	0	0	0	0	0	∞
Right	1.5	.81	13.01	10.21	47.55	-3.61	14.79	13.53	20.37	284.9
Right	2	.82	21.47	18.91	58.42	-10.23	25.43	15.63	31.55	183.9
Left	1.5	.79	13.03	-9.14	-47.35	-3.24	14.79	-13.62	-20.37	284.9
Left	2	.84	21.60	-18.14	-57.93	-9.83	25.41	-15.92	-31.55	183.9
$\gamma = 10°$										
--	0.9848	-9.31	10.54	0.89	0	0	0	0	0	∞
Right	1.5	-6.03	16.57	18.49	46.11	-6.64	14.30	13.76	20.93	273.0
Right	2	-4.71	24.31	28.68	55.89	-15.45	23.39	15.84	32.20	177.5
Left	1.5	-5.92	17.14	-6.61	-48.03	-2.41	15.46	-13.91	-20.93	273.0
Left	2	-4.52	26.29	-14.76	-58.68	-8.21	26.60	-16.19	-32.20	177.5
$\gamma = 20°$										
--	0.9397	-19.38	15.22	1.39	0	0	0	0	0	∞
Right	1.5	-12.81	20.48	27.54	43.55	-10.48	13.85	14.57	22.67	240.6
Right	2	-10.29	27.20	38.53	51.60	-21.32	20.98	16.63	34.23	159.3
Left	1.5	-12.70	22.35	-4.90	-49.13	-1.94	17.08	-14.78	-22.67	240.6
Left	2	-10.38	32.70	-12.99	-59.30	-7.69	28.67	-17.03	-34.23	159.3
$\gamma = -10°$										
--	0.9848	10.18	2.72	0.17	0	0	0	0	0	∞
Right	1.5	7.50	9.86	2.32	48.53	-0.85	15.67	13.85	20.93	273.0
Right	2	6.17	18.92	9.38	59.85	-5.25	27.47	15.96	32.20	177.5
Left	1.5	7.32	9.70	-12.45	-47.11	-4.51	14.97	-13.91	-20.93	273.0
Left	2	5.88	18.04	-22.66	-57.00	-12.41	24.92	-16.18	-32.20	177.5

TABLE 6.- Concluded.

Turn direction	Normal load factor, g	α, deg	β, deg	Θ, deg	Φ, deg	p, deg/sec	q, deg/sec	r, deg/sec	$\dot{\psi}$, deg/sec	Turn radius, ft
$\gamma = -20°$										
--	0.9397	19.99	-1.35	-0.01	0	0	0	0	0	∞
Right	1.5	13.79	7.00	-5.73	49.10	2.26	17.04	14.77	22.66	240.6
Right	2	11.20	16.76	.03	60.47	-.02	29.78	16.87	34.22	159.3
Left	1.5	13.42	7.04	-16.71	-47.06	-6.52	15.89	-14.79	-22.67	240.6
Left	2	10.54	15.37	-28.16	-55.71	-16.15	24.93	-17.00	-34.23	159.3

[a] V = 60 knots; gross weight = 2100 kg; middle center of gravity; sea-level standard day.

TABLE 7.- STABILITY AND CONTROL MATRICES OF THE HINGELESS-ROTOR HELICOPTER: V = 60 knots, $\gamma = 0°$

(a) Coordinated 1-g straight flight.

F matrix							
-0.32458E-01	0.28303E-01	0.16985E 01	-0.32199E 02	0.86781E-02	0.12926E 01	0.00000E 00	0.11487E 02
-.41619E-01	-.14181E 01	.10181E 03	-.25967E 00	-.12198E-01	-.81269E 01	.00000E 00	-.14694E 00
.13946E-01	.22968E-01	-.39935E 01	.00000E 00	-.27974E-02	-.29000E 00	.00000E 00	.11448E 00
.00000E 00	.00000E 00	.10000E 01	.00000E 00	.00000E 00	.00000E 00	.00000E 00	.00000E 00
-.72518E-02	-.10923E-01	-.51770E 00	.00000E 00	-.14334E 00	-.19082E 01	.32199E 02	-.99739E 02
-.54418E-02	-.22312E-01	-.58400E 01	.00000E 00	-.68990E-01	-.95784E 01	.00000E 00	.13466E 00
.00000E 00	.00000E 00	.00000E 00	.00000E 00	.00000E 00	.10000E 01	.00000E 00	.80645E-02
-.47220E-02	.76282E-02	.14407E 00	.00000E 00	.39663E-01	.48401E-01	.00000E 00	-.82685E 00

G matrix				
-0.74197E 00	0.13624E 00	-0.20831E-01	0.34340E-01	
-.22065E 01	-.93899E 01	.64059E 00	.36947E-01	V = 60 knots
.10223E 01	.27962E 00	.60630E-01	.27818E-01	$\gamma = 0°$
.00000E 00	.00000E 00	.00000E 00	.00000E 00	1 g
-.15533E-01	-.87421E-01	.71701E 00	-.17164E 01	$n_y = 0$
-.20508E 00	-.21598E 00	.23669E 01	-.10165E 01	
.00000E 00	.00000E 00	.00000E 00	.00000E 00	
-.33180E-01	.20991E 00	.32878E-01	.14528E 01	

Note: $\dot{\underline{x}} = F\underline{x} + G\underline{u}$; $\underline{x} = (u, w, q, \Theta, v, p, \Phi, r)^T$; $\underline{u} = (\delta_e, \delta_c, \delta_a, \delta_p)^T$.

Units = feet, radians, and seconds for state variables, inches for control variables.

TABLE 7.- Continued.

(b) Coordinated 2-g right turn.

F matrix							
-0.61211E-01	-0.45431E 00	0.39251E 01	-0.30461E 02	0.29569E 00	0.25300E 01	0.00000E 00	0.37047E 02
.31132E 00	-.14101E 01	.95375E 02	-.54663E 01	.13090E 00	-.34859E 02	-.25950E 02	-.17589E 00
.30873E-01	.26699E-01	-.45280E 01	.00000E 00	-.36134E-02	-.21770E 00	.00000E 00	-.42962E-01
.00000E 00	.00000E 00	.52370E 00	.00000E 00	.00000E 00	.00000E 00	-.52100E 00	-.85190E 00
-.29901E 00	-.19255E 00	-.11846E 01	-.88921E 01	-.17167E 00	-.42169E 01	.15952E 02	-.93452E 02
-.70642E-02	-.46093E-01	-.62172E 01	.00000E 00	-.11073E 00	-.11168E 02	.00000E 00	.30795E 00
.00000E 00	.00000E 00	.29192E 00	.58217E 00	.00000E 00	.10000E 01	.00000E 00	.17945E 00
-.87125E-02	.11244E-01	.14818E 00	.00000E 00	.36966E-01	-.26140E 00	.00000E 00	-.78742E 00
G matrix							
-0.15902E 01	-0.23456E 00	-0.29077E-02	0.73278E-01				
-.19302E 01	-.94279E 01	.10992E 01	.86118E-01	V = 60 knots			
.11731E 01	.32169E 00	.30663E-01	.69753E-01	$\gamma = 0°$			
.00000E 00	.00000E 00	.00000E 00	.00000E 00	2 g (R)			
.66388E-02	-.18949E 00	.14457E 01	-.18205E 01	$n_y = 0$			
-.16003E 00	-.46891E 00	.27420E 01	-.10782E 01				
.00000E 00	.00000E 00	.00000E 00	.00000E 00				
.37110E-01	.40550E 00	.98133E-02	.15410E 01				

Note: $\dot{\underline{x}} = F\underline{x} + G\underline{u}$; $\underline{x} = (u, w, q, \Theta, v, p, \Phi, r)^T$; $\underline{u} = (\delta_e, \delta_c, \delta_a, \delta_p)^T$.

Units = feet, radians, and seconds for state variables, inches for control variables.

TABLE 7.- Continued.

(c) Coordinated 2-g left turn.

F matrix							
-0.61458E-01	-0.45349E 00	0.39017E 01	-0.30600E 02	-0.25209E 00	0.28267E 01	0.00000E 00	0.37219E 02
.31132E 00	-.14092E 01	.95343E 02	.53234E 01	.12414E 00	-.34944E 02	.25929E 02	-.17184E 00
.31284E-01	.26328E-01	-.46111E 01	.00000E 00	-.51046E-02	-.75709E 00	.00000E 00	-.44888E-01
.00000E 00	.00000E 00	.53101E 00	.00000E 00	.00000E 00	.00000E 00	.52337E 00	.84737E 00
.24820E 00	-.18591E 00	-.83776E 00	-.84950E 01	-.17314E 00	-.40276E 01	.16249E 02	-.93341E 02
-.12527E-01	-.52348E-01	-.57379E 01	.00000E 00	-.11271E 00	-.10996E 02	.00000E 00	.32265E 00
.00000E 00	.00000E 00	.27762E 00	-.57954E 00	.00000E 00	.10000E 01	.00000E 00	-.17397E 00
-.75763E-02	.97914E-02	.13148E 00	.00000E 00	.38339E-01	-.23337E 00	.00000E 00	-.81144E 00

G matrix				
-0.15869E 01	-0.22441E 00	-0.63552E-01	0.86736E-01	
-.19394E 01	-.94195E 01	.10834E 01	.10513E 00	V = 60 knots
.11883E 01	.31868E 00	.82104E-01	.84333E-01	$\gamma = 0°$
.00000E 00	.00000E 00	.00000E 00	.00000E 00	2 g (L)
-.64266E-01	-.21047E 00	.14419E 01	-.18557E 01	$n_y = 0$
-.32032E 00	-.52936E 00	.27784E 01	-.10989E 01	
.00000E 00	.00000E 00	.00000E 00	.00000E 00	
.35097E-01	.40469E 00	.62055E-02	.15707E 01	

Note: $\dot{\underline{x}} = F\underline{x} + G\underline{u}$; $\underline{x} = (u, w, q, \Theta, v, p, \Phi, r)^T$; $\underline{u} = (\delta_e, \delta_c, \delta_a, \delta_p)^T$.

Units = feet, radians, and seconds for state variables, inches for control variables.

TABLE 7.- Continued.

(d) Uncoordinated 1-g straight flight: $n_y = 0.05$ (g).

F matrix							
-0.32490E-01	0.28388E-01	0.20920E 01	-0.32199E 02	-0.27553E-02	0.12857E 01	0.00000E 00	-0.76954E 01
-.42543E-01	-.14184E 01	0.10255E 03	-.24754E 00	0.32600E-03	0.11655E 02	0.16100E 01	-.13697E 00
.14097E-01	.23445E-01	-.39993E 01	.00000E 00	-.22457E-02	-.33033E 00	.00000E 00	.11580E 00
.00000E 00	.00000E 00	.99875E 00	.00000E 00	.00000E 00	.00000E 00	.00000E 00	.50001E-01
.93308E-02	-.81471E-02	-.60661E 00	.12393E-01	-.14355E 00	-.23074E 01	.32159E 02	-.10011E 03
-.40652E-02	-.21350E-02	-.59505E 01	.00000E 00	-.69291E-01	-.95896E 01	.00000E 00	.13122E 00
.00000E 00	.00000E 00	-.38488E-03	.00000E 00	.00000E 00	.10000E 01	.00000E 00	.76877E-02
-.53305E-02	.10953E-01	.18123E 00	.00000E 00	.40092E-01	.74302E-01	.00000E 00	-.82778E 00

G matrix				
-0.73798E 00	0.13615E 00	-0.81224E-02	0.24129E-01	
-.23140E 01	-.93904E 01	.26623E 00	.25808E-01	V = 60 knots
.10223E 01	.28437E 00	.64152E-01	.17034E-01	$\gamma = 0°$
.00000E 00	.00000E 00	.00000E 00	.00000E 00	1 g
-.79239E-02	-.37265E-01	.71510E 00	-.16886E 01	$n_y = 0.05$
-.18245E 00	-.31782E-01	.23646E 01	-.10001E 01	
.00000E 00	.00000E 00	.00000E 00	.00000E 00	
-.29659E-01	.21702E 00	.28280E-01	.14292E 01	

Note: $\dot{\underline{x}} = F\underline{x} + G\underline{u}$; $\underline{x} = (u, w, q, \Theta, v, p, \Phi, r)^T$; $\underline{u} = (\delta_e, \delta_c, \delta_a, \delta_p)^T$.

Units = feet, radians, and seconds for state variables, inches for control variables.

TABLE 7.- Continued.

(e) Uncoordinated 2-g right turn: $n_y = 0.05$ (g).

F matrix							
-0.62108E-01	-0.47197E 00	0.36357E 01	-0.31843E 02	0.29876E 00	0.25261E 01	0.00000E 00	0.16605E 02
.32636E 00	-.14138E 01	.10153E 03	-.25122E 01	.65921E-01	-.13501E 02	-.27097E 02	-.18180E 00
.30831E-01	.28748E-01	-.45628E 01	.00000E 00	-.29577E-02	-.25914E 00	.00000E 00	.67449E-02
.00000E 00	.00000E 00	.52520E 00	.00000E 00	.00000E 00	.00000E 00	-.54463E 00	-.85098E 00
-.29394E 00	-.86867E-01	-.12876E 01	-.40705E 01	-.17207E 00	-.38595E 01	.16724E 02	-.99151E 02
-.37634E-02	-.21854E-01	-.63401E 01	.00000E 00	-.11082E 00	-.11108E 02	.00000E 00	.23831E 00
.00000E 00	.00000E 00	.12783E 00	.55692E 00	.00000E 00	.10000E 01	.00000E 00	.78895E-01
-.10180E-01	.14095E-01	.77149E-01	.00000E 00	.37317E-01	-.27872E 00	.00000E 00	-.78304E 00

G matrix				
-0.15832E 01	-0.23245E 00	0.35306E-02	0.64351E-01	
-.21589E 01	-.94273E 01	.73377E 00	.77696E-01	V = 60 knots
.11758E 01	.34133E 00	.33863E-01	.59789E-01	$\gamma = 0°$
.00000E 00	.00000E 00	.00000E 00	.00000E 00	2 g (R)
.15472E-01	-.69835E-01	.14428E 01	-.17737E 01	$n_y = 0.05$ g
-.13797E 00	-.24389E 00	.27290E 01	-.10504E 01	
.00000E 00	.00000E 00	.00000E 00	.00000E 00	
.41838E-01	.40845E 00	.17976E-01	.15012E 01	

Note: $\dot{\underline{x}} = F\underline{x} + G\underline{u}$; $\underline{x} = (u, w, q, \Theta, v, p, \Phi, r)^T$; $\underline{u} = (\delta_e, \delta_c, \delta_a, \delta_p)^T$.

Units = feet, radians, and seconds for state variables, inches for control variables.

TABLE 7.- Continued.

(f) Uncoordinated 2-g left turn: $n_y = 0.05$ (g).

F matrix							
-0.62384E-01	-0.48573E 00	0.37020E 01	-0.31873E 02	-0.24848E 00	0.28239E 01	0.00000E 00	0.17264E 02
.33861E 00	-.14125E 01	.10144E 03	.22195E 01	.62326E-01	-.14091E 02	.27871E 02	-.17589E 00
.31246E-01	.29056E-01	-.46464E 01	.00000E 00	-.44544E-02	-.79733E 00	.00000E 00	-.23548E-02
.00000E 00	.00000E 00	.48516E 00	.00000E 00	.00000E 00	.00000E 00	.54515E 00	.87443E 00
.25272E 00	-.83454E-01	-.94352E 00	-.40003E 01	-.17250E 00	-.37576E 01	.15464E 02	-.99017E 02
-.92491E-02	-.28299E-01	-.58592E 01	.00000E 00	-.11212E 00	-.10933E 02	.00000E 00	.25459E 00
.00000E 00	.00000E 00	.12551E 00	-.55638E 00	.00000E 00	.10000E 01	.00000E 00	-.69635E-01
-.89323E-02	.12900E-01	.55882E-01	.00000E 00	.37906E-01	-.26235E 00	.00000E 00	-.79189E 00

G matrix				
-0.15814E 01	-0.23339E 00	-0.56866E-01	0.77742E-01	
-.21587E 01	-.94176E 01	.72508E 00	.96985E-01	V = 60 knots
.11916E 01	.34379E 00	.85141E-01	.74613E-01	$\gamma = 0°$
.00000E 00	.00000E 00	.00000E 00	.00000E 00	2 g (L)
-.54023E-01	-.90443E-01	.14391E 01	-.18084E 01	$n_y = 0.05$ g
-.29808E 00	-.30715E 00	.27651E 01	-.10710E 01	
.00000E 00	.00000E 00	.00000E 00	.00000E 00	
.43260E-01	.40894E 00	.14042E-01	.15306E 01	

Note: $\dot{\underline{x}} = F\underline{x} + G\underline{u}$; $\underline{x} = (u, w, q, \Theta, v, p, \Phi, r)^T$; $\underline{u} = (\delta_e, \delta_c, \delta_a, \delta_p)^T$.

Units = feet, radians, and seconds for state variables, inches for control variables.

TABLE 7.- Continued.

(g) Uncoordinated 1-g straight flight: $n_y = -0.05$ (g).

F matrix							
-0.31612E-01	0.29680E-01	0.23767E 01	-0.32195E 02	0.19456E-01	0.12906E 01	0.00000E 00	0.32051E 02
-.38088E-01	-.14155E 01	.96774E 02	-.57187E 00	-.25808E-01	-.29493E 02	-.16100E 01	-.15659E 00
.14055E-01	.20422E-01	-.39679E 01	.00000E 00	-.33560E-02	-.24406E 00	.00000E 00	.11537E 00
.00000E 00	.00000E 00	.99875E 00	.00000E 00	.00000E 00	.00000E 00	.00000E 00	-.50008E-01
-.24617E-01	-.13856E-01	-.44239E 00	-.28634E-01	-.14362E 00	-.26171E 01	.32155E 02	-.95146E 02
-.69622E-02	-.43857E-01	-.57477E 01	.00000E 00	-.69128E-01	-.95891E 01	.00000E 00	.15046E 00
.00000E 00	.00000E 00	.88939E-03	.00000E 00	.00000E 00	.10000E 01	.00000E 00	.17763E-01
-.39560E-02	.52501E-02	.88956E-01	.00000E 00	.40124E-01	.93248E-02	.00000E 00	-.84177E 00

G matrix				
-0.74616E 00	0.14868E 00	-0.30941E-01	0.44669E-01	
-.19986E 01	-.93907E 01	.10225E 01	.47813E-01	V = 60 knots
.10191E 01	.25829E 00	.56949E-01	.39249E-01	$\gamma = 0°$
.00000E 00	.00000E 00	.00000E 00	.00000E 00	1 g
-.19319E-01	-.14109E 00	.72063E 00	-.17503E 01	$n_y = -0.05$ g
-.22511E 00	-.41236E 00	.23771E 01	-.10366E 01	
.00000E 00	.00000E 00	.00000E 00	.00000E 00	
-.33773E-01	.21049E 00	.38131E-01	.14815E 01	

Note: $\dot{\underline{x}} = F\underline{x} + G\underline{u}$; $\underline{x} = (u, w, q, \Theta, v, p, \Phi, r)^T$; $\underline{u} = (\delta_e, \delta_c, \delta_a, \delta_p)^T$.

Units = feet, radians, and seconds for state variables, inches for control variables.

TABLE 7.- Continued.

(h) Uncoordinated 2-g right turn: $n_y = -0.05$ (g).

F matrix							
-0.55991E-01	-0.39501E 00	0.50550E 01	-0.27200E 02	0.28704E 00	0.25491E 01	0.00000E 00	0.61358E 02
.26988E 00	-.14022E 01	.80909E 02	-.96247E 01	.20806E 00	-.60499E 02	-.22563E 02	-.15752E 00
.30964E-01	.20669E-01	-.44621E 01	.00000E 00	-.41099E-02	-.18085E 00	.00000E 00	-.91821E-01
.00000E 00	.00000E 00	.55850E 00	.00000E 00	.00000E 00	.00000E 00	-.46523E 00	-.82950E 00
-.30386E 00	-.32045E 00	-.10909E 01	-.14295E 02	-.17623E 00	-.54948E 01	.15192E 02	-.79631E 02
-.10443E-01	-.75092E-01	-.61417E 01	.00000E 00	-.11273E 00	-.11309E 02	.00000E 00	.41739E 00
.00000E 00	.00000E 00	.52554E 00	.65197E 00	.00000E 00	.10000E 01	.00000E 00	.35384E 00
-.71184E-02	.80262E-02	.22391E 00	.00000E 00	.38828E-01	-.22952E 00	.00000E 00	-.83347E 00

G matrix				
-0.15969E 01	-0.19890E 00	-0.72225E-02	0.78061E-01	
-.15077E 01	-.94311E 01	.15015E 01	.86933E-01	V = 60 knots
.11658E 01	.26849E 00	.28778E-01	.77164E-01	$\gamma = 0°$
.00000E 00	.00000E 00	.00000E 00	.00000E 00	2 g (R)
.37354E-03	-.34284E 00	.14540E 01	-.18741E 01	$n_y = -0.05$ g
-.17541E 00	-.74948E 00	.27662E 01	-.11898E 01	
.00000E 00	.00000E 00	.00000E 00	.00000E 00	
.28592E-01	.40652E 00	.41323E-03	.15863E 01	

Note: $\dot{\underline{x}} = F\underline{x} + G\underline{u}$; $\underline{x} = (u, w, q, \Theta, v, p, \Phi, r)^T$; $\underline{u} = (\delta_e, \delta_c, \delta_a, \delta_p)^T$.

Units = feet, radians, and seconds for state variables, inches for control variables.

TABLE 7.- Concluded.

(i) Uncoordinated 2-g left turn: $n_y = -0.05$ (g).

F matrix							
-0.56587E-01	-0.38172E 00	0.49448E 01	-0.27709E 02	-0.26080E 00	0.28434E 01	0.00000E 00	0.60779E 02
.25914E 00	-.14023E 01	.81400E 02	.10069E 02	.19501E 00	-.59799E 02	.21873E 02	-.15814E 00
.31403E-01	.19388E-01	-.45511E 01	.00000E 00	-.56170E-02	-.72201E 00	.00000E 00	-.84570E-01
.00000E 00	.00000E 00	.61391E 00	.00000E 00	.00000E 00	.00000E 00	.47393E 00	.78938E 00
.24443E 00	-.30640E 00	-.73960E 00	-.12947E 02	-.17946E 00	-.52219E 01	.17011E 02	-.79992E 02
-.15469E-01	-.80368E-01	-.56635E 01	.00000E 00	-.11567E 00	-.11138E 02	.00000E 00	.43039E 00
.00000E 00	.00000E 00	.46726E 00	-.63999E 00	.00000E 00	.10000E 01	.00000E 00	-.36339E 00
-.66461E-02	.61649E-02	.20319E 00	.00000E 00	.41545E-01	-.19437E 00	.00000E 00	-.88287E 00

G matrix				
-0.15925E 01	-0.17758E 00	-0.68348E-01	0.92219E-01	
-.15368E 01	-.94222E 01	.14787E 01	.10595E 00	V = 60 knots
.11808E 01	.26036E 00	.80450E-01	.91846E-01	$\gamma = 0°$
.00000E 00	.00000E 00	.00000E 00	.00000E 00	2 g (L)
-.71431E-01	-.36065E 00	.14512E 01	-.19089E 01	$n_y = -0.05$ g
-.33552E 00	-.79213E 00	.28051E 01	-.11304E 01	
.00000E 00	.00000E 00	.00000E 00	.00000E 00	
.23401E-01	.40452E 00	-.22477E-02	.16159E 01	

Note: $\dot{\underline{x}} = F\underline{x} + G\underline{u}$; $\underline{x} = (u, w, q, \Theta, v, p, \Phi, r)^T$; $\underline{u} = (\delta_e, \delta_c, \delta_a, \delta_p)^T$.

Units = feet, radians, and seconds for state variables, inches for control variables.

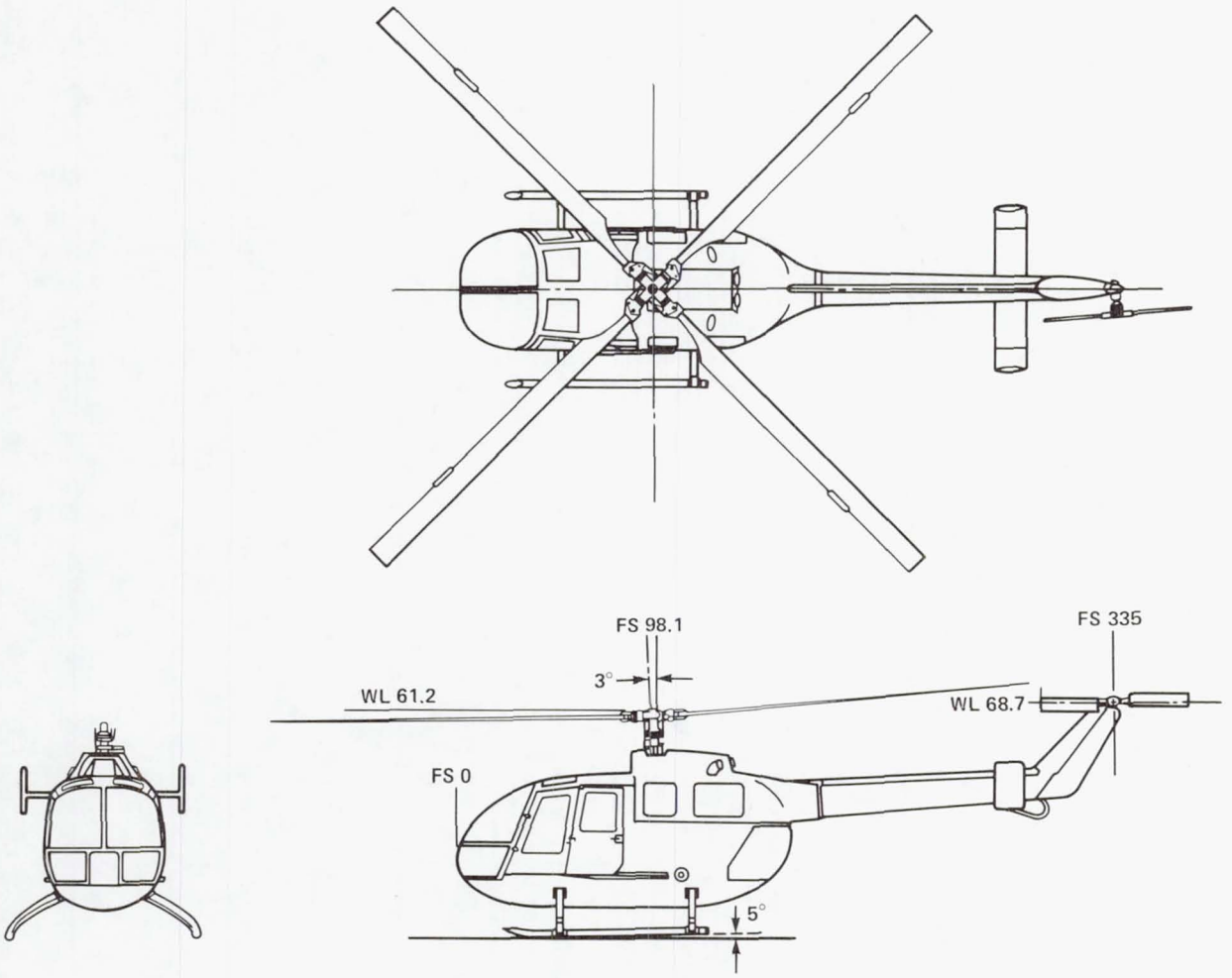

Figure 1.- BO-105C (from ref. 21).

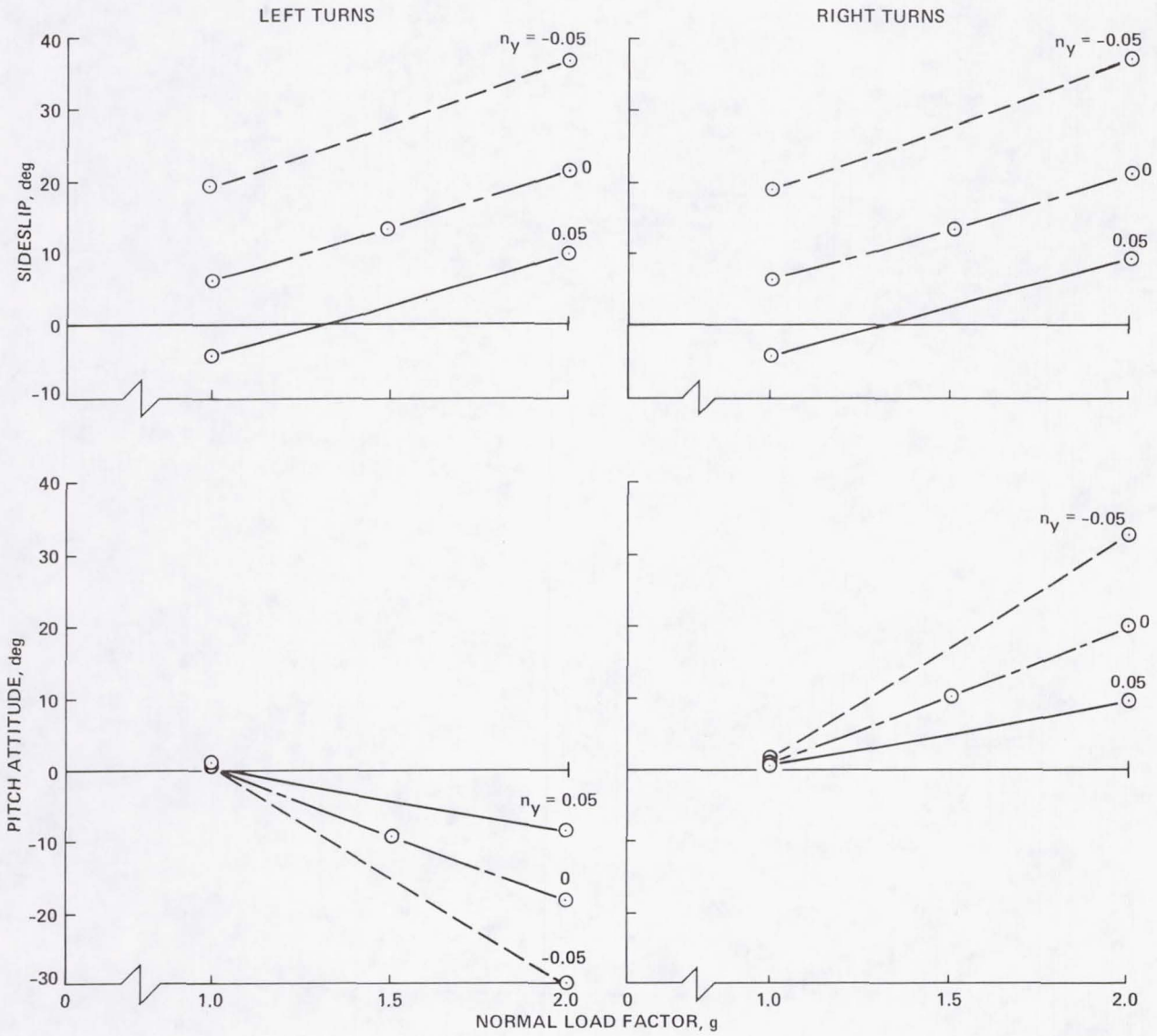

Figure 2.- Effect of being out-of-coordination on static characteristics of a simulated hingeless-rotor helicopter in steady turn, V = 60 knots, γ = 0°.

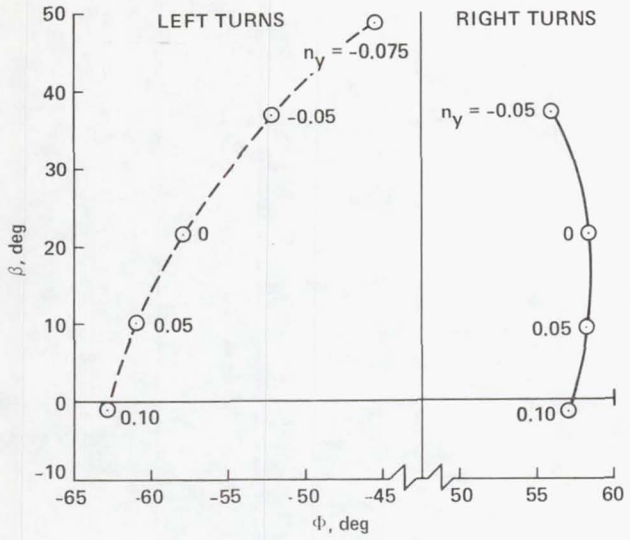

Figure 3.- Effect of being out-of-coordination on $\beta - \Phi$ relationship of a hingeless-rotor helicopter in steady level turns: V = 60 knots, $\gamma = 0°$, $n_T = 2$.

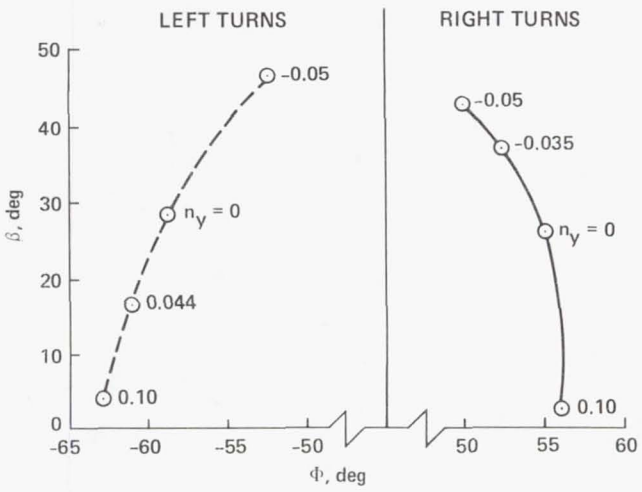

Figure 4.- Effect of being out-of-coordination on $\beta - \Phi$ relationship of a hingeless-rotor helicopter in steady climbing turns: V = 60 knots, $\gamma = 10°$, $n_T = 2$.

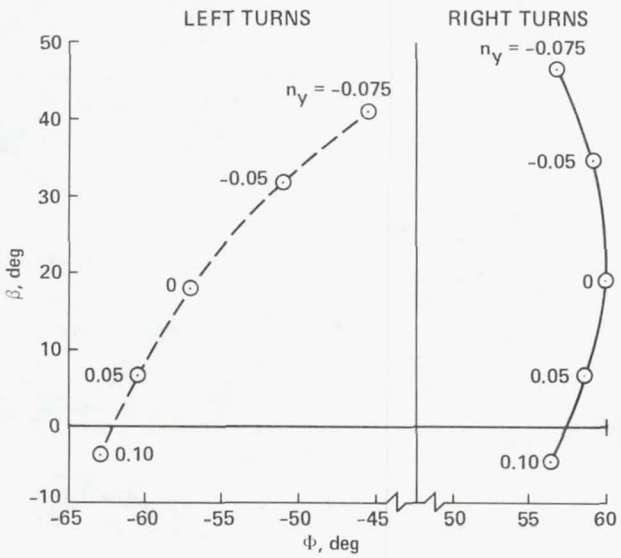

Figure 5.- Effect of being out-of-coordination on $\beta - \Phi$ relationship of a hingeless-rotor helicopter in steady descending turns: V = 60 knots, $\gamma = -10°$, $n_T = 2$.

1. Report No.	2. Government Accession No.	3. Recipient's Catalog No.
NASA TM-84324		

4. Title and Subtitle	5. Report Date
EFFICIENT ALGORITHMS FOR COMPUTING TRIM AND SMALL-DISTURBANCE EQUATIONS OF MOTION OF AIRCRAFT IN COORDINATED AND UNCOORDINATED, STEADY, STEEP TURNS	6. Performing Organization Code

7. Author(s)	8. Performing Organization Report No.
Robert T. N. Chen	A-9220
	10. Work Unit No. T6292
9. Performing Organization Name and Address	11. Contract or Grant No.
NASA Ames Research Center Moffett Field, Calif. 94035	
	13. Type of Report and Period Covered
12. Sponsoring Agency Name and Address	Technical Memorandum
National Aeronautics and Space Administration Washington, D.C. 20546	14. Sponsoring Agency Code 505-42-11

15. Supplementary Notes

Point of Contact: Robert T. N. Chen, Ames Research Center, MS 211-2, Moffett Field, CA 94035. (415) 965-5008 or FTS 448-5008.

16. Abstract

The development of computational algorithms that permit efficient calculation of aircraft trim states and of the associated small-disturbance equations of motion for a systematic investigation of the statics and dynamics of aircraft in coordinated and uncoordinated, steady, steep-turning flight is reported. The efficiency in the trim computation is realized by decoupling the governing equations. The small-disturbance equations of motion, which are given in a general body-axis system, include aerodynamic acceleration derivatives; they are cast in a familiar first-order, vector-matrix format of modern system theory. These algorithms have been applied to a variety of rotorcraft simulation models. Results pertaining to a simulated hingeless-rotor helicopter are also presented.

17. Key Words (Suggested by Author(s))	18. Distribution Statement
Helicopter flight simulation Flight dynamics Coordinated or uncoordinated turns Trim algorithm Stability and control	Unlimited Subject Category - 08

19. Security Classif. (of this report)	20. Security Classif. (of this page)	21. No. of Pages	22. Price*
Unclassified	Unclassified	40	A03

*For sale by the National Technical Information Service, Springfield, Virginia 22161